FOUR TRANSDUCER ULTRASONIC ARRAY FOR DETECTING AND SIZING DEFECTS IN PLATE AND PIPE MATERIALS

G. J. Posakony and T. T. Taylor

Pacific Northwest Laboratory
Automation and Measurement Sciences Department
Richland, Washington 99352

INTRODUCTION

Ultrasonic pulse-echo techniques are widely used for detection and sizing of defects. However, studies over recent years have shown that the detection and sizing capability of many of the widely accepted ultrasonic techniques do not provide accuracy required to assure safety, reliability or maintainability. While certain types and orientations of defects can be detected, others may go undetected. Even after detection, studies have shown that the ability to size defects is far from accurate. [1,2,3]

Significant research has gone into the development and improvement of techniques and procedures for sizing of defects. Tip diffraction [4,5,6] and time of flight (TOF) [7,8] provide a substantial improvement over amplitude based sizing techniques. [9] However, for tight cracks or randomly oriented defects, the tip diffraction and TOF signals are often difficult to identify, thus reducing the reliability of these techniques. Focused probes provide an enhanced means for sizing defects; however, specially designed probes are often required for each type or depth of defect. [9,10,11] Ultrasonic synthetic aperture and holographic imaging techniques have provided further improvements over manual or automated pulse echo procedures and are an important means for providing detail of critical defects. [12,13] The principal drawbacks to the imaging procedures are cost and availability of equipment and time required to perform the procedure. Imaging techniques are generally more effective for thicker wall piping and pressure vessel structure.

FOUR TRANSDUCER ARRAY

Pacific Northwest Laboratory (PNL), operated by Battelle Memorial Institute, has developed a four transducer ultrasonic array network designed to detect and size randomly oriented defects in heat exchanger tubing. A particular goal of the development was to determine the through wall penetration of surface connected defects or internal inclusions that might be present in the tube. The nominal diameter of the tubing is 3.25 inches (82.5 mm) with a wall thickness of 0.27 inches (6.9 mm).

One of the criteria of design for the four transducer array inspection station was that all data must be collected automatically in a single pass through the heat exchanger tube. Due to the nature of the inspection, it was not practical to re-enter the tube for detailed scanning and signal analysis. Typical defects expected in the tube included, surface connected ID and OD cracks, laminations, weld defects, fretting, wall thinning and tube ovality. Defects could be at any orientation. The four transducer array combined information from amplitude, time and spatial recording position to develop defect data. Special emphasis was placed on development of a means for reducing the responses from surface scratches that were known to be present in the tube, but which were not considered detrimental to tubing integrity.

PRINCIPLE OF OPERATION

The four transducer array is shown in Figure 1. The information available from the four transducer array includes:

A. Pulse-transmission energy between transducer #1 and #4 [AMPLITUDE AND SPATIAL POSITION]
B. Diffracted and mode converted energy from tube OD conditions (Transducer #2) [AMPLITUDE AND SPATIAL POSITION]
C. Diffracted and mode converted energy from tube ID conditions (Transducer #3) [AMPLITUDE AND SPATIAL POSITION]
D. Diffracted, reflected and mode converted energy from center wall conditions. [e.g. inclusions, voids and weld conditions] (Transducers #2 and #3) [AMPLITUDE, TIME AND SPATIAL POSITION]
E. Water path distance to validate coupling, fretting depth and measure ovality. (Transducer #3) [TIME AND SPATIAL POSITION]
F. Wall thickness to measure corrosion, erosion and depth of inclusions. (Transducer #3) [TIME AND SPATIAL POSITION]
G. Pulse-echo reflections from OD, ID or mid-wall defects. (Transducer #1, #3 and #4) [AMPLITUDE, TIME AND SPATIAL POSITION]

It is evident that a great deal of information can be obtained from various combinations of available data. From a practical standpoint, it was established that data from any single channel must be validated by data from one or more channels before it was accepted for analysis.

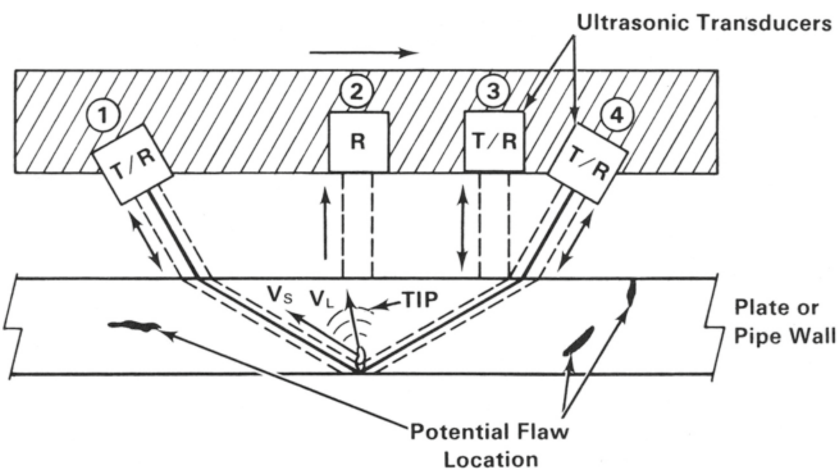

Fig. 1. Four transducer array configuration.

THEORY OF OPERATION

Four modes, or responses (reflected, transmitted, mode converted and diffracted energies), are available. In addition, the spatial position of the array in the tube provides size and location information. Consideration was also given to the size and frequency of the transducers, the directivity function (size and orientation) of the potential flaws and the nature of the flaws (cracks, inclusions, etc.) that were anticipated to reside in the tube.

For the four transducer array, the pulse-echo transducers (#1 and #4) were designed for 60 degree shear wave inspection. The size of the transducers was 0.365 inch (9.5 mm) and the operating frequency was 4 MHz. The size and frequency were chosen to maximize the response from mode converted and diffracted responses associated with flaws, defects, and scratches. The procedures used for detecting and characterizing defects are discussed later.

Reflected

The pulse-echo energy reflected from a defect provides amplitude and time information. This is the conventional inspection procedure used for ultrasonic examinations. As previously indicated, the amplitude of energy reflected from a defect is critically dependent on the orientation of the defect.

Transmitted

In the transmitted mode, the energy is projected into the tube from transducer #1, reflected from the back wall and received by transducer #4. Any defect that interrupts the sound beam, regardless of orientation or position within the tube wall, decreases the amount of energy received by the receiving transducer. The amount of energy loss is nearly linear from about one wavelength to the size at which the sound beam and the defect are of nearly equal dimensions.

The location of the defect within the tube wall can be determined by the spatial location of the transducers (Figure 2). A defect at Position 1 will interrupt the sound beam between the ID and OD surfaces. The sound beam will be interrupted again between the OD and ID surfaces as the array is indexed for inspection of the tube (Position 2). Since

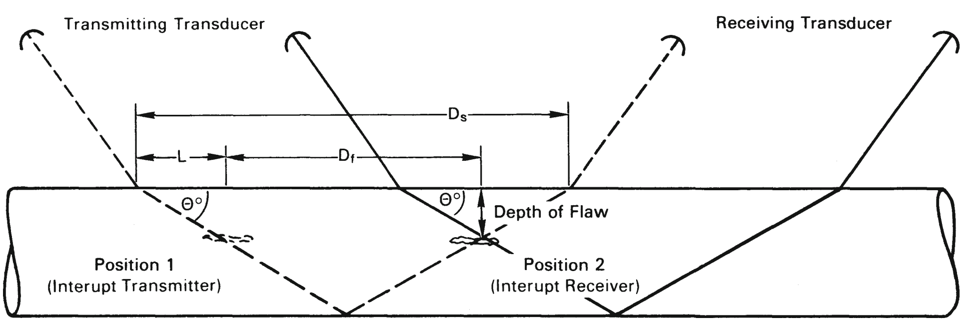

$$L = \frac{D_s - D_f}{2}$$

Depth of Flaw = tan Θ x L

Fig. 2. Triangulation for location (depth) calculation.

the transducers are fixed in the water filled probe head, the depth can be determined by measuring the distance D_f and triangulating for the through wall dimension. A difference in depth below the surface is a direct function of the distance D_f.

Mode Converted

The four transducer array is uniquely different from other arrays in that the design is configured for maximum use of mode converted energy from defects. The 60 degree, shear wave sound beam, incident on a defect, will reflect a shear wave beam and will convert part of the sound energy from shear to longitudinal. Figures 3A and 3B show two of the possible patterns. Figure 3A sketches the sound beam reflecting from the back wall and interacting with the defect. Figure 3B shows the sound beam reflecting from the defect and interacting with the back wall. These mode converted patterns (also known as Delta conversions) [14] are valid for sound beam incident angles below the critical angle. Transducers #2 and #3 (See Figure 1) are used to receive the mode converted energies.

The critical angle for steel, as determined by Snell's Law, can be calculated from: [15]

$$\frac{\text{SIN } \theta_L}{\text{SIN } \theta_S} = \frac{V_L}{V_S} \qquad \text{OR} \qquad 1.82 \text{ SIN } \theta_S = \text{SIN } \theta_L$$

For Delta mode conversions, calculations show that shear wave insonification should lie between 55 and 65 degrees. While this appears to be a relatively limited range, a review of Figures 3A and 3B reveals that the angle of the defect can be significantly greater and still provide an excellent signal response from the mode converted energy. Since the flaw may be illuminated by either the reflection from the back wall or the reflection from the defect, angulation of the flaw actually expands the range over which mode conversions occur. As an example, in Figure 3A, a defect that lies ten degrees from the normal will result in the mode converted signal exiting the steel at an angle near normal to the surface. Since the defect may be viewed from two directions, the potential for producing a mode converted signal from off axis defects is enhanced.

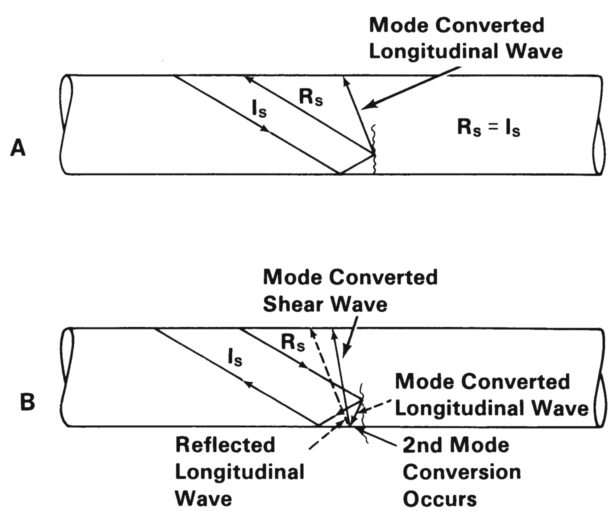

Fig. 3. A and B: Mode converted signal sources.

Experimentation has established that a strong mode converted signal is produced from defects that are as much as ± 20 degrees from normal incidence at either the OD or ID surfaces. Further, the defect orientation can be in either the X or Y planes (Z being distance) without substantial decrease in the Delta response. Thus, the mode converted energy is relatively insensitive to defect orientation.

The operating frequency was chosen to reduce the signal response from scratches in the 0.01 inch (0.25 mm) range. The wavelength of a 4 MHz shear wave beam in steel is 0.02 inch (0.8 mm). Below a wavelength there is little mode converted energy. Above about a wavelength, the amount of received energy is nearly linear with defect size until the size of the defect reaches the size of the sound beam.

Diffraction

Diffraction occurs at the edges of flaws and defects. The tip diffraction techniques [4,5,6] can be used to measure through-wall dimensions. Likewise, the diffraction signals can be and are detected by Transducers #2 and #3 (See Figure 1). While tip diffraction signals may be detected, the automated inspection system used by PNL for the heat exchanger examination did not use this information for sizing. The presence of the diffracted signal, particularly from mid-wall defects such as inclusions, provides additional information for flaw characterization.

EXPERIMENTAL RESULT

Some of the results obtained with the four channel array are shown in Figure 4. The figure shows amplitude response for the transmission and mode converted energy recorded for a series of EDM notches in a steel test plate. It also shows the plot of the amplitude of the mode converted energy (Delta) reflected from EDM notches in the calibration test plate, and the associated response from the same notches for energy transmitted through the notched zone.

As shown in Figure 4, the Delta response is linear to approximately 0.1 inch, then it falls off as the notch size increases. This condition is attributable to the

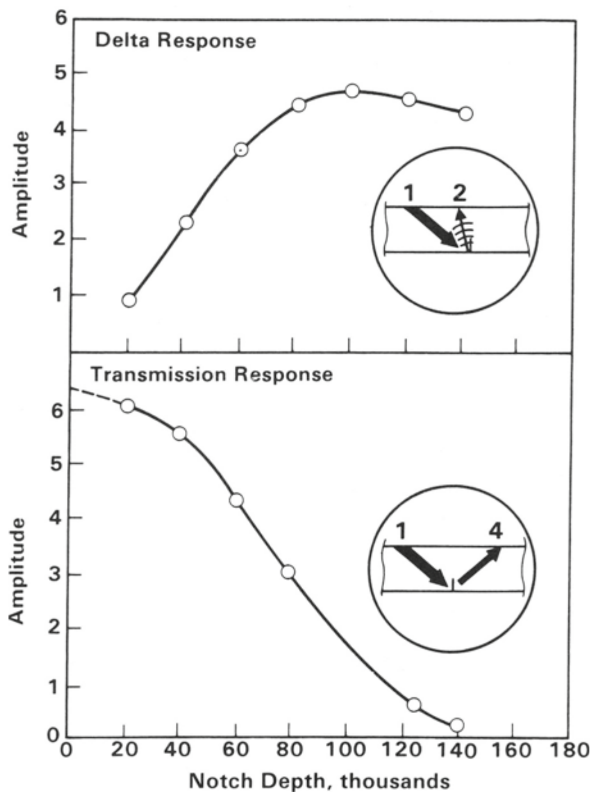

Fig. 4 Response from the four transducer array.

size of the insonifying beam. The linear range can be extended by increasing the size of the beam. The same phenomena is observed in the pulse-echo procedure. The transmission response decreases with notch depth. As with the Delta response, the size of the sound beam controls the depth through which the response is linear. To obtain size information, the response from both the Delta response and the transmission response must be used. As with the Delta response, the transmission response is also insensitive to defect orientation. Neither response, by itself, provided the required data.

Non-surface connected defects, such as inclusions or weld defects, may obtain data from the transmission or Delta response modes and/or data may be added from other transducers in the array. As an example, an inclusion may provide two responses in the transmission mode, one in the thickness mode, one in the pulse echo mode, and energy is often observed in the ID or OD Delta channels.

A wealth of data is available from the four transducer array. Figure 5 provides some insight into the amount and complexity of the information. The drawing shows the type of information that is recorded on the strip chart from a flat bottomed hole (FBH) that is machined half way through the tube wall.

Channel #1 is the water couplant channel. Loss of couplant, presence of air in the couplant water and presence of tube ovality are shown in this channel.

Channel #2 records the depth of the defect in the tube. The spatial position (number of times recorded) defines the length of defect and the size (circumfrential) is defined by the width of the step. Spatial position provides lengths and circumfrential dimension.

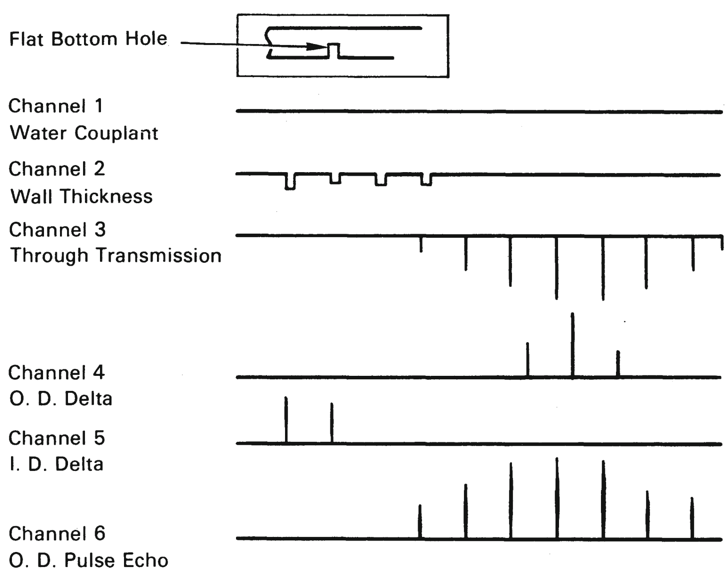

Fig. 5. Strip chart record.

Channel #3 shows the loss of energy from transducer #1 to #4. The information is spaced at a different location from channel # 2 as the array was at a different location during this portion of the inspection procedure. If the chart were continued, the transmission channel would show a second pattern of information and depth could also be verified from these data. (See Figure 2 - Triangulation)

Channel #4 shows that information is available from the base of the FBH. The position on the strip chart, related to the transmission data, confirms the source of the data.

Channel #5 is from the wave that is mode converted from the side of the FBH or diffracted from the top edge of the hole. The location under the information from channel 2 helps verify the size and nature of the defect.

Channel #6 is the pulse echo response. This is typical of what should be received from a FBH. Its location and response pattern should be expected. While the pulse echo is apparently effective for the FBH, the pulse echo mode is very critical to orientation.

The data provided on the strip chart and the knowledge of the indexing of the sonde are used to accurately size the defect. As an example, in Figure 5, the sonde increments 0.075 inch (1.9 mm) after each rotation. Since the FBH is recorded on four successive rotations, its diameter would be measured as 0.3 inch (7.6 mm). The actual size of 0.25 inch (6.35 mm) would be determined by subtracting the effective size of the sound beam. The depth of the FBH is recorded in channel 2. The recording shows a depth of 0.106 (2.67 mm) versus actual of 0.1 (2.54 mm). In channel #2 off-angle inclusions may have shown as loss of back. These data combined with information from other channels, provides ability to size defects.

CONCLUSIONS

The four transducer ultrasonic array developed by PNL provided an automated, non-imaging, system for detecting and sizing defects in tubing and plate. By combining amplitude information with time and spatial position, and by using a combination of records for defect characterization, a reliable and repeatable inspection was performed.

Destructive/nondestructive correlation on actual defects has been limited (four specimens); however, results from both crack-like defects and inclusions have been very encouraging. In the instance of an angled inclusion, where no data appeared in the pulse-echo channel, the size, orientation and location were predicted within 10% of the actual dimension. In other instances, the ability to characterize the difference between a crack-like defect and an inclusion proved valuable to the fracture mechanics calculations.

The technology associated with the four transducer array network is still under development and further refinement is planned in both the optimization of the sound beams and in analysis procedures. However, the amount of data available with the technology provides a strong basis for developing a data acquisition and analysis system that can detect, locate, size and characterize defects. Because data from multiple sound beams are recorded, and because each channel of data provides a unique amount of information, there is an opportunity for automating the analysis procedure thorough the use of expert systems and neural networks.

REFERENCES

1. T.T. Taylor, P.G. Heasler, and D.J. Bates, "An Evaluation of Current Capabilities in Characterization of Intergranular Stress Corrosion Cracking," in 8th International Conference on NDE in the Nuclear Industry.
2. S. Crutzen, P. Jehenson, R. Nichols, and N. McDonald, "From Capability Evaluation to Reliability Assessments: A Review of the PISC Projects". Organisation for Economic Co-operation and Development, Nuclear Energy Agency, PISCDOC(87)26, November 1987.
3. W.D. Rummel, 1984. Assessment of NDI Reliability on Engine Components During Overhaul. Martin Marietta Corporation Report, Contracts F41608-79-D-A064 and F41608-82-D-A070, Denver, Colorado.
4. M.G. Silk and B.H. Lidington, British Journal of NDT, March 1975.
5. K.E. Lindenschmidt and M.D.C. Moles - "Sizing Cracks in Candu Reactor Pressure Tubing Using Crack Tip Diffraction." - No. 87-276-K, Ontario Hydro Research Division, Toronto, Canada, Dec. 1987.
6. G.J. Gruber, "Defect Identification and Sizing by the Ultrasonic Satellite-Pulse Technique," in Proceedings of the 9th Nuclear Power Education Seminar, SWRI, San Antonio, Texas, April 23-26, 1979.
7. J.A.G. Temple, - "Estimating the Depth of Intergranular Attack by Ultrasonic Time-Delay." AERE R 12141 - United Kingdom Atomic Energy Limited, Harwell Laboratory, Oxfordshire OX11 ORA, November 1987.
8. M.G. Silk, "Sizing of Cracks by Ultrasonic Means. Research Techniques in Nondestructive Testing", R.S Sharpe, Editor, Volume III, 1976, pp. 51-99.
9. A.J. Willetts, F.V. Ammirato, and E.K. Keitzman - "Accuracy of Ultrasonic Flaw Sizing Techniques for Reactor Pressure Vessels." Interim Report - RP 1570-2, EPRI, Palo Alto, California, March 1988.
10. F. Waite and W. Muller, - "Influence of Crack Inclination and Roughness on the Ultrasonic Inspection Using Focussed Sound Probes." IZFP, Saarbrucken, Federal Republic of Germany.
11. R. Saglio, A.M. Birac, J.C. Frappier, and R. Lefevre, "Systeme de Traitement et d'Acquisition de Donnees Ultrasonores," in Proceedings of the 5th International Conference on NDE in Nuclear Industries, San Diego, California, May 1982.
12. S.R. Doctor, T.E. Hall, and L.D. Reid, "Real-Time SAFT-UT for Nuclear Component Inspection", in Proceedings from 8th International Conference on NDE in the Nuclear Industry.
13. B.P. Hildebrand, "Stepped Frequency Ultrasonic Holography for Flaw Characterization", 11th World Conf. on NDT, 1985. Vol. II, p. 971.
14. G.J. Posakony and B.T. Cross, U.S. Patent No. 3,712,119, Jan. 1973.
15. J. Krautkramer and H. Krautkramer - Ultrasonic Testing of Materials Springer - Verlag, Inc., New York, New York, 1969.